Al-Khwarizmi Engineering Journal
ISSN (printed): 1818 – 1171, ISSN (online): 2312 – 0789
Vol. 20, No. 1, March, (2024), P. P. 1- 16

Al-Khwarizmi Engineering Journal

Modification, Characterization of Tea Residue-derived Activated Carbon, and Ciprofloxacin Adsorption

Alaa Kareem Mohammed* Israa M. Rashid Nadya Hussin AL Sbani*** Wan Nor Roslam Wan Isaha******

,Department of Biochemical Engineering / Al-Khwarizmi College of Engineering/ University of Baghdad/ Baghdad / Iraq*

****Department of Chemical Engineering/ Faculty of Oil and Gas Engineering/ Al Zawia University/ Libya*

*****Department of Chemical and Process Engineering/ Faculty of Engineering and Built Environment/ Universiti Kebangsaan Malaysia/ 43600 UKM Bangi/ Selangor/ Malaysia*

Corresponding Author*Email: dr.alaa@kecbu.uobaghdad.edu.iq

**Email: israa msc2018@kecbu.uobaghdad.edu.iq

***Email: n.alsbani@zu.edu.ly

****Email: wannorroslam@ukm.edu.my

(Received 29 August 2023; Accepted 6 November 2023; Published 1 March 2024)

https://doi.org/10.22153/kej.2024.11.001

Abstract

Tea residue was used for preparing activated carbon (AC) which was used as an adsorbent to remove Ciprofloxacin (CIP) from synthetic contaminated water. This study investigates the physicochemical properties and adsorption efficiency of the prepared activated carbon. The activated carbon was prepared via two steps: Activation step using phosphoric acid (H_3PO_4) followed by carbonization at a temperature of 450 °C. Different factors were investigated to show their effects on the adsorption efficiency of (CIP). These factors were initial concentration of (CIP), pH, Absorption time, and adsorbent dosage. The maximum adsorption efficiency was 94.4% which was obtained when pH=8.75, contact time =454 min, adsorbent dosage =0.194 g/ 25 ml, and initial concentration of 200 ppm. The prepared activated carbon was characterized using Fourier transform infrared spectroscopy (FTIR), scanning electron microscopy (SEM), X-ray diffraction (XRD), and Brunauer-Emmett-Teller (BET). The prepared activated carbon was found to have a specific surface area of 774 m^2/g. It was found that the Langmuir model well fit the adsorption isotherm of (CIP) on the prepared activated carbon. The produced activated carbon can adsorb Ciprofloxacin, with a maximum adsorption capacity of 256.41 mg g^{-1}. A pseudo-second-order reaction model is effective at describing the kinetics of adsorption. The examination of adsorption thermodynamics reveals that the process of CIP adsorption on TAC is characterized by being both endothermic and spontaneous.

Keywords: *Adsorption, Tea residue, Active carbon, Ciprofloxacin, adsorption kinetics, adsorption thermodynamics.*

1. Introduction

Water is essential to human life and the health of the environment. Its existence is described as a limiting factor for human development. The growing population demands more water for a wide range of uses while water resources are limited. In addition to that, the rapid increase in industrial and human activities produces increasing amounts of waste matter as well as a higher spread of environmental water pollution [1]. Pollution, in its broadest sense, includes all changes that restrict natural functions and exert damaging effects on life [2]. Water pollution is the undesired change in water quality that leads to an unfavorable alteration of the physical, chemical, and biological properties of water that prevents domestic, commercial, industrial, agricultural, recreational, and other beneficial uses of water [3], [4]. There are various types of water pollutants; they are mainly

categorized into organic pollutants (e.g., petroleum hydrocarbons, aromatic hydrocarbons, organic halides, oils, dyes, etc.), and inorganic compounds (e.g., mineral acids, inorganic salts, trace elements, metal compounds, cyanides, sulfate, heavy metals, etc. [5], [6]. Veterinary medicine, human medicine, and the pharmaceutical industries are the principal contributors of pharmaceutical residues to the environment. In addition, when therapeutic compounds are discharged from factories, hospitals, and private homes or when unwanted pharmaceuticals are improperly disposed of, surface water and groundwater are contaminated, and drinking water is contaminated as a result. This poses a potential health risk to humans [7]. As a result, many treatment technologies have been proposed to treat this type of wastewater, such as reverse osmosis, ion exchange, adsorption, and nanofiltration [8]. Among these methods, the adsorption process is regarded as a promising method for the removal of micropollutants because of its simple design, low cost, high efficiency, and low production of toxic intermediates [9]. Due to antibiotics' toxicological effects on aquatic species and the resistance they can create in some bacterial strains, even at low concentrations, the presence of antibiotics in surface water and wastewater has been regularly reported and is growing in importance. [10].

Ciprofloxacin (CIP; $C_{17}H_{18}O_3N_3F$) is efficient against several different Gram-negative and Gram-positive bacteria [11]. CIP is frequently detected in groundwater and polluted wastewater as a result of its widespread use to treat several human and animal illnesses. [12]. Figure 1 shows the basic structure of CIP.

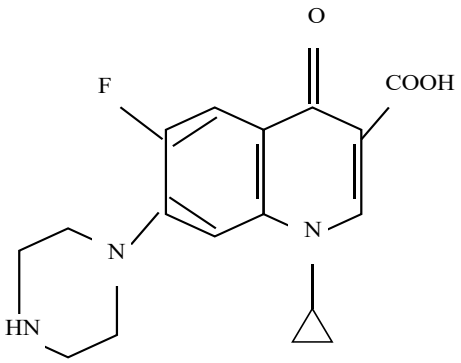

Fig. 1. Structure of Ciprofloxacin.

Several adsorbents, as cheap and efficient alternate materials, have been used, such as activated carbon, graphene, and silica, for water purification [13], [13]. A wide range of inorganic and organic pollutants are removed from the aquatic environment and industrial wastewater using activated carbon as an efficient adsorbent due to its high surface area, porosity structure, the presence of a broad spectrum of surface functional groups, and the capability of pollutant distributed on the high internal surface [14]. Activated carbon is widely used as an adsorbent due to its features such as low cost, availability, and surface heterogeneity [15]. Therefore, the practical usage of AC is restricted by the price of precursors and relatively high preparation costs [16]. Biomass waste as a renewable resource has attracted widespread attention. Aiming to reduce the total cost regarding the preparation of AC, using biomass waste as a precursor of AC, including groundnut husks [17], sugarcane bagasse [18], coconut shells [19], and tea residue [20], [21], is a viable option. Apart from the precursors, the physicochemical property of AC is also associated with the preparation method. The preparation of AC is divided into the following two methods, i.e., chemical activation and physical activation [22]. Typically, the activation temperature for lignocelluloses, precursors of AC, is between 800 and 1000 °C. During the chemical activation stage, acid, alkali, and salt, such as phosphoric acid (H_3PO_4) [20], potassium hydroxide (KOH) [15], and zinc chloride ($ZnCl_2$) [23], are often employed as activating agents. Activating temperature, impregnation ratio, and activation time[24], [25] are some of the factors that affect the physicochemical properties of AC during the chemical activation process.

This study was concerned with the feasibility of using tea residue as a low-cost and readily available sorbent material for the removal of Ciprofloxacin from aqueous solutions in batch mode. Tea residue was selected as a precursor to prepare activated carbon using chemical activation with H_3PO_4. The adsorption of Ciprofloxacin was also looked at to find out about the adsorption equilibrium, kinetics, and thermodynamics of the AC sample that was made.

2. Materials and Methods

2.1 Materials

The tea residue was collected locally from leftover tea used in homes. Ciprofloxacin (CIP) was chosen as the target adsorbate and supplied by the Ministry of Health, Iraq. Ciprofloxacin was directly used without any further treatment. Phosphoric acid (H_3PO_4), used as the activating agent, was purchased from Himedia, India.

2.2 Preparation of activated carbon

The waste tea was boiled with distilled water for 2 hours to remove water-soluble materials and then washed with distilled water until the washing water was colorless. The decolorized waste tea was dried in a drying oven at 110 °C for 10 hours. Before activation, the waste tea was fully mixed with a 60% (by wt) H_3PO_4 solution at an impregnation ratio of 1:2.5 (g waste tea /g H_3PO_4) at room temperature for 12 hours. The mixture was then filtered. After pretreatment, the raw material was placed in a closed steel crucible for carbonization in a furnace at 450 °C for 1 hour with nitrogen. The N_2 flow is 150 cm^3/min. After cooling to room temperature, the activated carbon was washed with distilled water (DW) until pH equaled seven. Then the carbons were dried at 110 °C for 6 hours. The product (TAC) was ground with mortar and sieved to obtain a particle size equal to or less than 350 µm then preserved in a desiccator for the upcoming batch trials.

2.3 Activated Carbon Characteristics

Various characterizations were performed to describe the adsorbent produced. Scanning electron microscopy (SEM) was used to analyze the surface morphologies (JOEL, JSM-7600 F, Tokyo, Japan). Fourier transform infrared spectroscopy (FTIR 8400s Shimadzu) was used to study the functional groups on the adsorbent surface using KBr pellets in the (4000-400 cm^{-1}) range. X-ray diffraction (XRD) was used to determine the crystalline phase (type Shimadzu XRD 6000 / Japan). The elemental composition of the absorbent was studied using EDX (JOEL, JSM-7600 F, Tokyo, Japan). The Brunauer-Emmett-Teller (BET) analysis (HORIBA, SA-900 series, USA), to determine the surface area and porous structure of activated carbon.

2.4 Ciprofloxacin Adsorption on TAC

At room temperature, batch adsorption experiments with 50 ml of Ciprofloxacin (CIP) solution were carried out at different initial concentrations (100–500 mg/l), pH (2–11), contact time (15-600 min), and active carbon (TAC) dosage (0.025–0.25 g/25 ml) at a constant speed of agitation (150 rpm). In the Erlenmeyer flask (250 ml), 50 ml of CIP solution of the specified initial concentration was put in. The TAC was added with a known quantity and mixed well at 150 rpm using an orbital shaker(Edmund Buhler SM25, German).

After that, the adsorbent was removed from the aqueous solution using filter paper (Whatman). The final CIP concentration was measured using a double-beam UV-visible spectrophotometer (PG Instruments, Model UV T80, England). The CIP has a wavelength of 272.5 nm. The proportion of CIP removed by the prepared activated carbon (TAC) was calculated using Eq. (1) [26].

$$\boldsymbol{R}\ \% = \left[\frac{\boldsymbol{C_0 - C_e}}{\boldsymbol{C_0}}\right] * \mathbf{100}\% \qquad \ldots(\mathbf{1})$$

Where R represents the removal percentage, C_o & C_e are initial and equilibrium concentrations of CIP (mg/l) respectively. The adsorption capacity at equilibrium q_e was calculated using Eq.(2) [27], [28].

$$\boldsymbol{q}_e = \frac{(\boldsymbol{C_0 - C_e})\boldsymbol{V}}{\boldsymbol{m}} \qquad \ldots(\mathbf{2})$$

Where V(ml) is the sample volume and m (g)is the adsorbent quantity.

2.5 Design of an Adsorption Experiment

The central composite Design (CCD) was used in the experimental design with four variables at five levels. These variables were: Adsorption time, solution acidity pH, adsorbent dosage, and CIP initial concentration Co. These variables were studied to investigate their impact on the adsorption efficiency of CIP. To design, analyze, and optimize the influencing parameters as well as to create an empirical model illustrating the CIP's adsorption efficiency, experimental design software (CCD) was employed.

The independent factors, with their actual levels and coding chosen for process optimization, are shown in Table 1.

Table 1,
Adsorption experimental design following CCD

Run	X_1: Adsorption time (min)	X_2: pH	X_3: Dosage (g/25ml)	X_4:sa Initial Conc. (mg/L)	R% (Experimental)	R% Predicted	Residuals
1	307.5	6.5	0.1375	100	86.86	87.05	-0.1854
2	161.25	8.75	0.08125	200	77.1	77.05	0.0529
3	453.75	8.75	0.08125	400	77.6	77.61	-0.0137
4	161.25	4.25	0.19375	200	83	82.91	0.0913
5	307.5	6.5	0.1375	300	80	80	0
6	307.5	6.5	0.1375	500	74.2	74.26	-0.0571
7	161.25	8.75	0.19375	400	78	78.09	-0.0887
8	161.25	4.25	0.19375	400	83	82.92	0.0792
9	453.75	4.25	0.08125	400	77	77	-0.0008
10	453.75	4.25	0.19375	400	82	81.98	0.0246
11	307.5	6.5	0.25	300	87	87.09	-0.0871
12	161.25	4.25	0.08125	200	75.6	75.56	0.0358
13	307.5	2	0.1375	300	80	80.12	-0.1171
14	15	6.5	0.1375	300	76.5	76.66	-0.1604
15	161.25	8.75	0.19375	200	84	83.83	0.1658
16	453.75	8.75	0.19375	400	82.16	82.03	0.1292
17	161.25	8.75	0.08125	400	71.03	70.87	0.1558
18	453.75	8.75	0.08125	200	90.5	90.41	0.0858
19	600	6.5	0.1375	300	89	89.08	-0.0821
20	307.5	6.5	0.025	300	75.17	75.33	-0.1554
21	453.75	8.75	0.19375	200	*94.4*	*94.41*	*0.0063*
22	161.25	4.25	0.08125	400	75.22	75.15	0.0713
23	453.75	4.25	0.19375	200	88.6	88.59	0.0092
24	453.75	4.25	0.08125	200	84.21	84.04	0.1663
25	307.5	6.5	0.1375	300	80	80	0
26	307.5	6.5	0.1375	300	80	80	0
27	307.5	11	0.1375	300	81.53	81.66	-0.1254

The effects of the parameter on CIP sorption were modeled and designed using the CCD method, as illustrated in Table 1. The time for absorption (X_1), pH (X_2), dose of the adsorbent (X_3), and CIP's initial concentration (X_4) were used to optimize the response removal of CIP (R%). The value of the coefficient of determination R^2 was used to assess the fit of the regression, Eq. (3), and it was found to be 0.9997, approving the model's accuracy.

$$R = 80 + 3.11\,X_1 + 0.3846\,X_2 + 2.94X_3 - 3.2\,X_4 + 1.22\,X_1X_2 - 0.6994\,X_1X_3 - 1.66\,X_1X_4 - 0.1394\,X_2X_3 - 1.44\,X_2X_4 + 0.1069\,X_3X_4 + 0.7178\,{X_1}^2 + 0.2216\,{X_2}^2 + 0.3016\,{X_3}^2 + 0.1628\,{X_4}^2 \quad \ldots(3)$$

Figure 2 plots the predicted vs. observed values of removal percent content in the five-factor CCD analysis. The predicted responses from the empirical function are almost identical to the measured values, where all points are close to the line in the range of the operating factors.

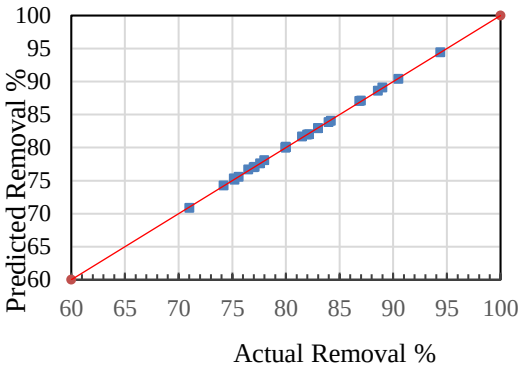

Fig. 2. Predicted vs. actual values of the percentage removal of CIP adsorption.

3. Results and Discussion

3.1 Characterization of the activated carbon

3.1.1 Characterization using FT-IR

The chemical structure of the carbon substance is revealed through infrared spectroscopy. Figure 3

shows the FTIR spectra of the synthetic carbons obtained by phosphoric acid activation at different concentrations. A broad transmittance band is visible in all spectra between 3200 and 3600 cm^{-1}, with maxima at roughly 3420 to 3440 cm^{-1}. The O-H stretching mode of the hydroxyl groups and the adsorbed water can be attributed to this band. All carbons' spectra have a faint, acute transmittance band between 2921 and 2855 cm^{-1}, which decreases when carbons are exposed to high concentrations of H_3PO_4 [29]. The spectral bands shown in Figure 3 at wavenumbers 885, 840, and 775 cm^{-1} can be attributed to the out-of-plane deformation mode of the C-H bonds in different substituted benzene rings. The spectral feature observed at approximately 1700 cm^{-1} is commonly attributed to the stretching vibrations of C-O bonds in ketones, aldehydes, lactones, or carboxyl groups. The activated carbons that were synthesized exhibit a prominent spectral feature in the range of 1600-1580 cm^{-1}, which can be attributed to the vibrations of carbon-carbon bonds inside aromatic rings. The spectral peak observed at the wavenumber range of 1190-1200 cm^{-1} has been attributed to the stretching mode of hydrogen-bonded P=O, as well as the stretching vibrations of O-C bonds in P-O-C (aromatic) linkages. Additionally, this peak is also associated with the presence of P=OOH. This assignment is supported by reference [30].

In summary, the analysis of impregnation in infrared spectroscopy (IR) reveals significant alterations, notably the introduction of phosphorous groups (at a wavenumber of 1100 cm^{-1}) and the emergence of C-H vibrations. The latter can be attributed to the depletion of oxygen at the carbon material's surface.

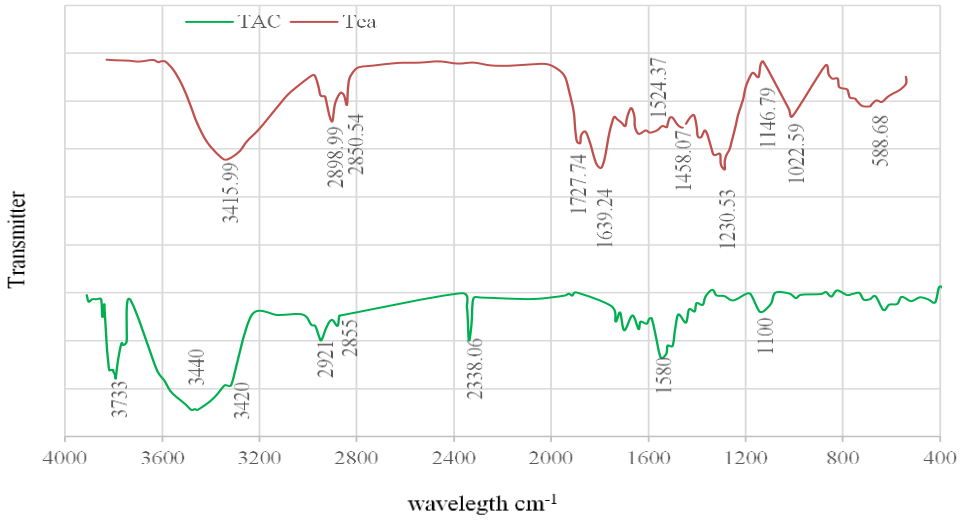

Fig. 3. FTIR spectra of the raw material, tea residue, and tea active carbon TAC.

3.1.2 Characterization using SEM

The prepared active carbon's (TAC) form and surface morphology were investigated using SEM and EDX analysis, as illustrated in Figure 4. Figure 4a which illustrates the micro-surface morphologies of (TAC). The activated carbon depressions exhibit internal structures characterized by the presence of cavities and cracks on their external surfaces. The presence of holes on carbon surfaces can be attributed to the evaporation of the activating agent, phosphoric acid, during the carbonization process. This evaporation leads to the creation of voids in the areas formerly occupied by the agent. [31]. The H_3PO_4 impregnation, followed by a heat treatment in an inert environment, affects the microstructure of activated carbon. These effects will break down many of the bonds within the material and thus lose many of the components that make up the material, which will lead to an increase in pores within the material. The elemental analysis of activated carbon was conducted using energy-dispersive X-ray spectroscopy (EDX), as shown in Figure 4b, and indicates the existence of carbon at 69.66 %, oxygen at 16.89%, nitrogen at 12.06 %, and phosphorus at 1.48%

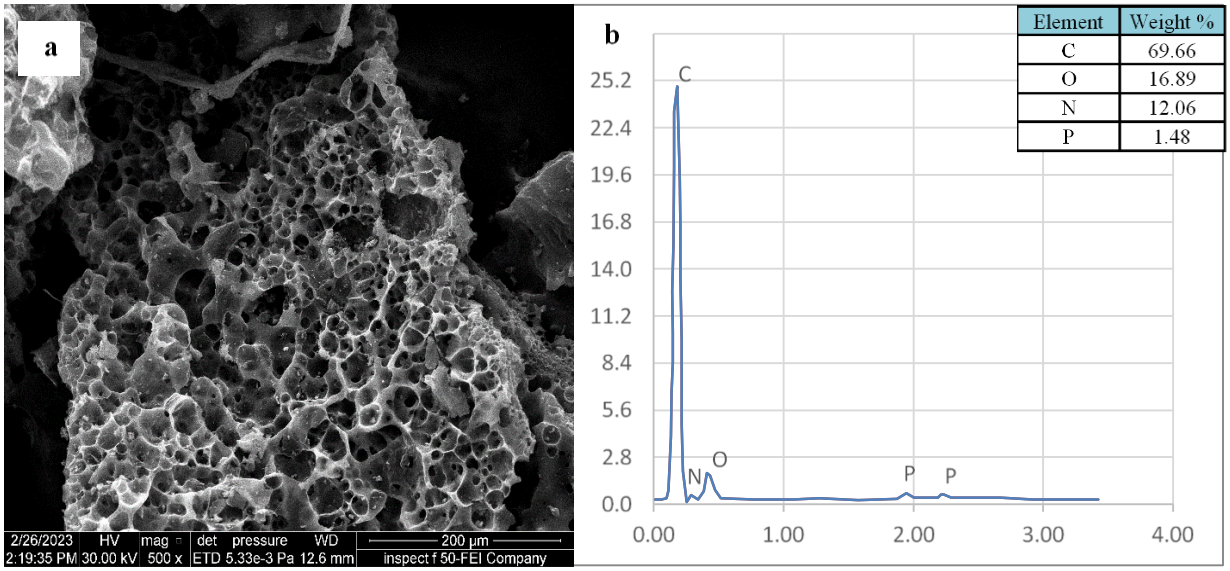

Fig. 4. (a) SEM image of Active carbon, (b) EDS spectra of TAC.

3.1.3 Surface Area and Pore Structure

The results of the Brunauer-Emmett-Teller (BET) research revealed that the activated carbon derived from tea residue (TAC) exhibited a specific surface area of 774 m^2/g and an average pore volume of 0.563 cm^3/g. These results are consistent with the findings of Tao et al. [15] who prepared activated carbon from tea residue and found the surface area and pore size fall in the range of 503-1337 m^2/g and 0.353-0.817 cm^3/g, respectively. Also, Tuli et al. [32] found that the surface area and pore size of the activated carbon were 850.58 cm^3/g and 0.67 cm^3/g, respectively.

3.2 ANOVA analysis

Table 2 presents the empirical outcomes of the analysis of variance (ANOVA) assessments. The statistical significance of a parameter is indicated by its corresponding p-value. The model's F-value of 2592.2 and p-value of less than 0.0001 indicate that the model is statistically significant. In this case, X_1, X_2, X_3, X_4, X_1X_2, X_1X_3, X_1X_4, X_2X_3, X_2X_4, X_3X_4, X_1^2, X_2^2, X_3^2, and X_4^2 are significant model terms. Values greater than 0.05 indicate the model terms are not significant. The analysis results in Table 2 indicate the significant effect of each variable in the model on removal efficiency. It can be observed that the initial concentration C_o parameter in the linear form X_4 (F-value = 11012.55) has the most significant effect on removal efficiency, followed by the linear term of the mixing time X_1 (F-value = 10390.10). In interactive terms, the most significant effective parameters are pH and initial concentration X_2X_4 (F-value = 1488.12), and the other is mixing time and initial concentration X_1X_4 (F-value = 1971.82), as well as mixing time and dosage X_1X_3 (F-value = 1072.36).

Table 2,
ANOVA Results of CIP Adsorption Findings.

SOURCE	SUM OF SQUARES	MEAN SQUARE	F-VALUE	P-VALUE	
MODEL	808.4	57.74	2592.2	< 0.0001	significant
X_1-TIME	231.45	231.45	10390.1	< 0.0001	significant
X_2-PH	3.55	3.55	159.35	< 0.0001	significant
X_3-DOSAGE	207.51	207.51	9315.32	< 0.0001	significant
X_4-CO	245.31	245.31	11012.55	< 0.0001	significant
X_1X_2	23.89	23.89	351.32	< 0.0001	significant
X_1X_3	7.83	7.83	1072.36	< 0.0001	significant
X_1X_4	43.92	43.92	1971.82	< 0.0001	significant
X_2X_3	0.3108	0.3108	13.95	0.0028	significant
X_2X_4	33.15	33.15	1488.12	< 0.0001	significant
X_3X_4	0.1828	0.1828	8.2	0.0142	significant
X_1^2	10.99	10.99	493.46	< 0.0001	significant
X_2^2	1.05	1.05	47.01	< 0.0001	significant
X_3^2	1.94	1.94	87.09	< 0.0001	significant
X_4^2	0.5655	0.5655	25.39	0.0003	significant
RESIDUAL	0.2673	0.0223			
PURE ERROR	0	0			
COR TOTAL	808.67				

An analysis of variance (ANOVA) was employed to evaluate the appropriateness of the model. The quadratic model was found to be very significant, with the values of R-squared, adjusted R-squared, and predicted R-squared correlation coefficients equal to 0.9997, 0.9993, and 0.9981, respectively. This value indicates the proportionality of the experimental values and the predicted adsorption removal values. The ANOVA analysis of CIP adsorption nearly agrees with that of [7], who studied the removal of diclofenac from aqueous solution on apricot seeds using activated carbon synthesized by pyrocarbonic acid microwave and analyzed the results using the Response Surface Methodology method.

3.3 Interactions of Adsorption Parameters

3.3.1 pH and initial concentration of CIP

Figure 5 shows the 3D response surface and contours of how the most important factors, pH and the initial concentration of CIP, interact. The p-value and F-value are indicators of these outcomes, as shown in Table 2. Figure 5 shows that the initial concentration is the most important factor in the adsorption process. In the range of the initial concentration of CIP (Co) between 100 and 500 ppm, the adsorption percentage increased with increasing pH. The observed phenomena can be attributed to the competitive interaction between CIP and H+ ions for adsorption sites, occurring on the surface of the adsorbent under conditions characterized by low pH levels. The adsorbent exhibits a progressive increase in adsorption capacity as the pH level rises, eventually reaching its peak adsorption efficiency of 94.4% at a pH of 8.75 and an initial concentration of 200 ppm. Nevertheless, when the pH is equal to 11, the adsorption capacity of TAC fibers exhibits a little drop. This can be attributed to the weakening of hydrogen bonding caused by the presence of OH^{-1} ions. This behavior aligns with the findings of Haotian et al., who conducted a study on the adsorption of tetracycline antibiotics. [33].

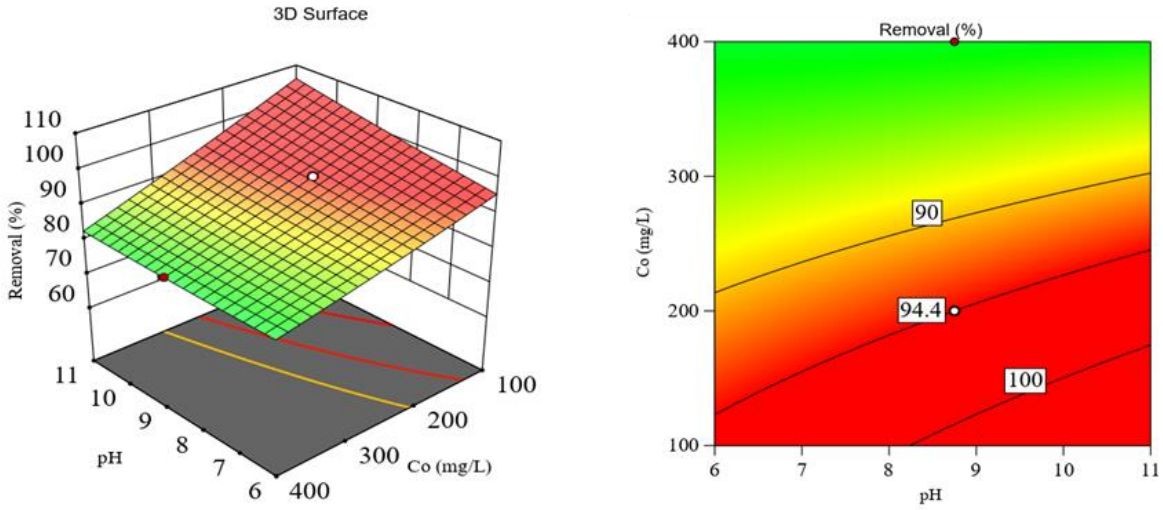

Fig . 5. Counter plots and 3D of removal percent (%) of CIP as a function of pH and initial concentration of CIP (ppm).

3.3.2 Adsorption time and initial concentration of CIP

The influence of adsorption time on the CIP ions adsorbed by TAC was investigated and presented in Figure 6. The P-value and F-value are indicators of these outcomes, as shown in Table 2. Figure 6 shows that the adsorption time is the most important factor in the absorption process. When the initial concentration of CIP (Co) was between 100 and 200 ppm, increasing the adsorption time led to a higher percentage of CIP being removed. When the concentration of CIP is greater than 200 ppm, the adsorption capacity gradually slows down over time. This observation is due to the fact that the increasing concentration requires more time to be adsorbed. This behavior is in agreement with [10]. The optimum values for mixing time and initial concentrations are 454 min and 200 ppm, respectively.

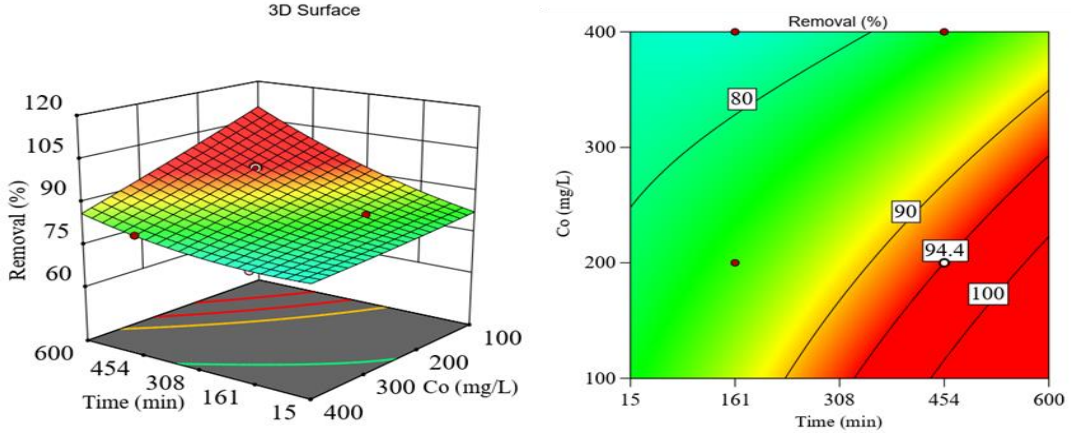

Fig. 6. Counter plots and 3D of removal percent (%) of CIP as a function of time (min) and initial concentration of CIP (ppm).

3.3.3 Mixing time and TAC dosage

The effects of contact time and TAC dosage on the removal efficiency of CIP using TAC were studied in the ranges 15 - 600 min and 0.025 - 0.25 g / 25ml, respectively. The results are shown in Figure 7. This indicates that the removal efficiency is increased by increasing the contact time and TAC dosage until the values of the removal efficiency become constant. The optimum values for mixing time and TAC dosage are 454 min and 0.194 g / 25ml, respectively. These results are in agreement with the findings of [34].

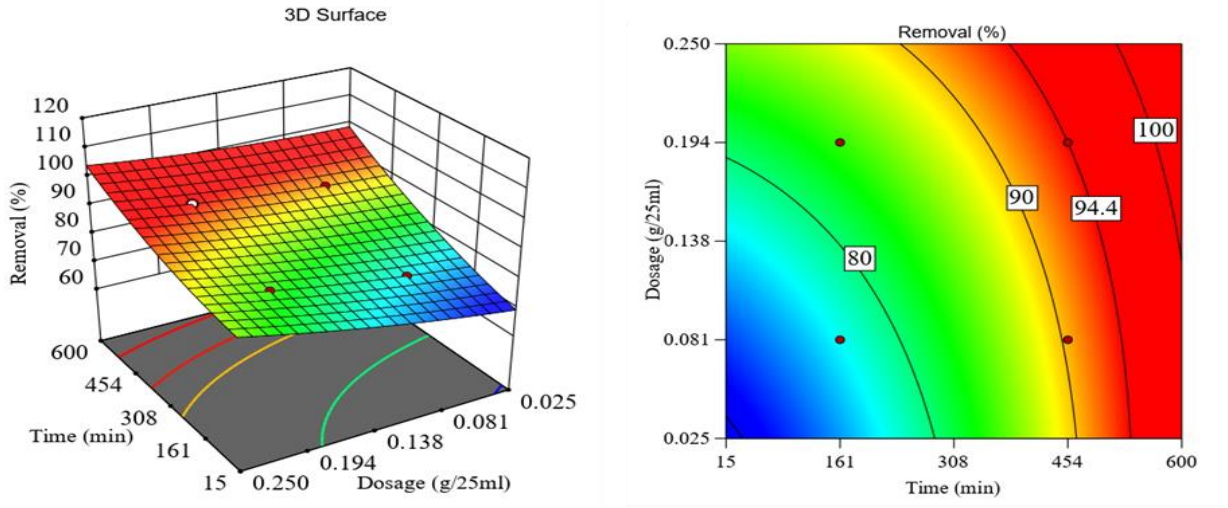

Fig. 7. Counter plots and 3D of removal percent (%) of CIP as a function of time (min) and TAC dosage (g/25ml).

3.4 Optimization of process variable

The model accuracy was validated by optimizing the process parameters of the adsorption of CIP on TAC. The experimental result obtained confirmed the validity of the model, as shown in Table 3, with 94% removal.

Table 3,
Adsorption of CIP on TAC optimization following the designed model.

Process Parameters (Coded)	Time	pH	Dosage	C_o	Predicted R^2	Actual R^2	Error %
Optimal Values	454	8.75	0.194	200	0.9993	0.9981	0.0012

4. Adsorption Isotherms

Adsorption isotherms, which are essential for creating adsorption systems, are calculated using equilibrium data. Figure 8 illustrates how two linearized isotherm models (Langmuir and Freundlich) are used to match the sorption data for CIP. Consequently, the slope and intercept of the linear plot were employed to determine the empirical coefficients presented in Table 4 for each model. Eq. (4) represents the Langmuir isotherm [35].

$$q_e = \frac{K_L\, q_m\, C_e}{1 + K_L C_e} \quad \ldots (4)$$

The linearized form of Eq. (4) is given by Eq. (5)

$$\frac{1}{q_e} = \frac{1}{q_m} + \frac{1}{q_m K_L}\,\frac{1}{C_e} \quad \ldots (5)$$

Where

q_e adsorption capacity at equilibrium (mg/g).
q_m : Maximum adsorption capacity (mg/g).
K_L : Constant (L/mg).
C_e : The equilibrium concentration of the (mg/L).

Equation (5) can be used to determine both K_L and q_m. The Freundlich model is based on the assumption of multi-layer adsorption and heterogeneous surface energies. Equation (6) represents the Freundlich isotherm [23].

$$q_e = K_F C_e^{\frac{1}{n}} \quad \ldots (6)$$

Eq. (7) represents the linearization form of the Freundlich model

$$\ln(q_e) = \ln(K_F) + \frac{1}{n}\ln(C_e) \quad \ldots (7)$$

The parameters n and K_F are Freundlich constants, which represent the adsorption intensity and the adsorption capacity, respectively. Equation (7) is used to determine the values of n and K_F. Figure (8) shows the fitting of both models Langmuir and Freundlich.

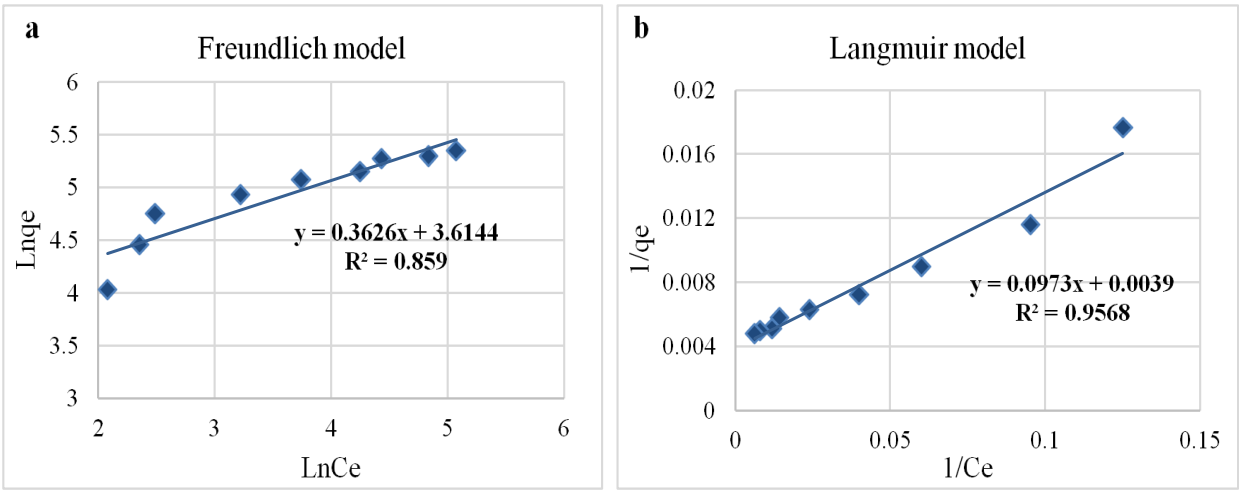

Fig. 8. Linear form of the Freundlich and Langmuir isotherm models for the sorption of CIP onto TAC.

Table 4 shows the parameters of both models Langmuir and Freundlich as well as the correlation coefficient (R^2).

Table 4,
Parameters of Langmuir and Freundlich equations

Freundlich			Langmuir		
K_F	n	R^2	K_L (L/mg)	q_m (mg/g)	R^2
37.13	2.76	0.859	24.95	256.41	0.9568

According to the correlation coefficient values (R^2), the Langmuir model matches the experimental results more closely than the Freundlich model, which predicts a high monomolecular layer on the surface of the TAC.

5. Kinetics Adsorption

Two kinetic models were used to analyze the adsorption kinetics of CIP onto TAC to comprehend the regulating mechanism and the adsorption rate: pseudo-first-order and pseudo-second-order as represented by Equations (8) and (9), respectively. [36], [37].

$$\left(\frac{dq_t}{dt}\right) = K_1\,(q_e - q_t) \quad \ldots (8)$$

$$\frac{dq_t}{dt} = K_2(q_e - q_t)^2 \quad \ldots (9)$$

The parameters q_t and q_e (mg/g) represent the amounts of the TC adsorbed on the TAC at time t and equilibrium, respectively. K_1(min^{-1}) and $K_2\,(g/mg.min)$ represent the rate constants of the pseudo-first-order and pseudo-second-order kinetics, respectively.

Eqs. (10) and (11), respectively, give the linearized forms of the pseudo-first-order and pseudo-second-order [38].

$$ln(q_e - q_t) = \ln q_e - K_1 t \quad \ldots (10)$$

$$\frac{t}{q_t} = \left(\frac{1}{K_2 {q_e}^2}\right) + \left(\frac{t}{q_e}\right) \quad \ldots (11)$$

The experimental adsorption data are graphically presented in Figure 9 using the pseudo-first-order and pseudo-second-order kinetics models.

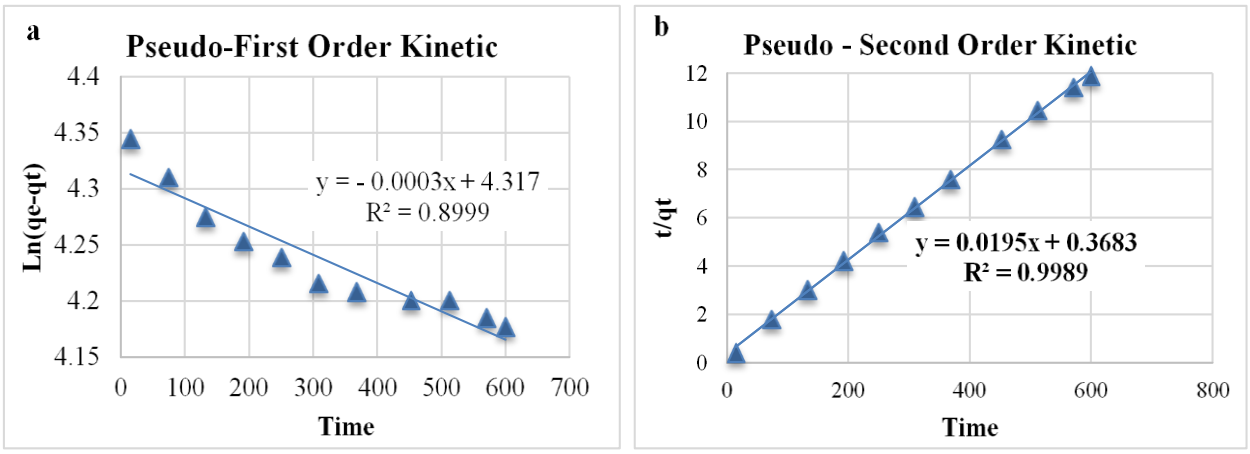

Fig. 9. Kinetics models for adsorption of CIP onto TAC. (a) Pseudo-first-order, (b) Pseudo -second-order reaction model.

Table 5,
Kinetics parameters of pseudo-first-order and pseudo-second-order adsorption models

Pseudo-first-order			Pseudo-second-order		
K_1 (min^{-1})	q_e (mg/g)	R^2	K_2 (g/mg. min)	q_e (mg/g)	R^2
0.0003	74.96	0.8999	0.001	51.282	0.9989

Table 5 shows that the pseudo-second-order kinetic well fits the experimental data of CIP adsorption on the TAC.

6. Study of Thermodynamics

Three thermodynamic parameters, including, entropy change ΔS^0, Gibbs free energy change ΔG^0, and enthalpy change ΔH^0, were studied to investigate the thermodynamic behavior of the adsorption onto the TAC. The Gibbs free energy change ΔG^0, was determined by Eq. (12) [39].

$$\Delta G^o = RTln(K_c) \quad \text{... (12)}$$

Where R is the universal gas constant ($R = 8.314\, kJ/kmol.K$) and K_c is the distribution coefficient that can be calculated by Eq. (13) [40].

$$K_c = \frac{q_e}{C_e} \quad \text{... (13)}$$

The relation between the thermodynamic parameters enthalpy change ΔH^o, entropy change ΔS^o, and Gibbs free energy change $\Delta G^o$is given by Eq. (14) [41].

$$\Delta G^o = \Delta H^o - T\Delta S^o \quad \text{... (14)}$$

Substituting Eq. (14) in Eq. (12) gives

$$\ln K_c = \frac{\Delta S°}{R} - \frac{\Delta H°}{RT} \quad \text{... (15)}$$

The values of ln(K_c) were calculated by Eq. (13) at different temperatures. Plotting ln(K_c) vs. $\frac{1}{T}$ gives a linear relation from which the values of ΔH^o and ΔS^o can be calculated. Figure 9 illustrates a positive correlation between the value of Kc and temperature, indicating that when the temperature rises, Kc also increases. Table 6 presents a comprehensive overview of the thermodynamic parameters $\Delta G°, \Delta H°,$ and $\Delta S°$ at various temperatures for the adsorption of CIP onto TAC.

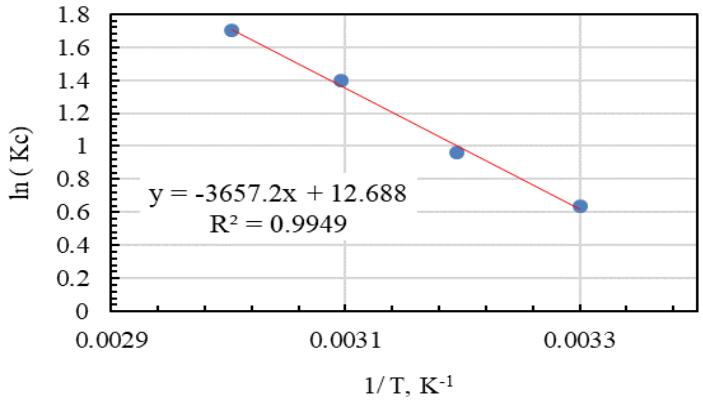

Fig. 9. ln K_c versus $\frac{1}{T}$ for the adsorption of CIP on TAC.

Table 6,
Thermodynamic parameters for the adsorption of CIP by the Active Carbon

ΔG^o (kJ/mol)				ΔS^o(kJ/mol K)	ΔH^o (kJ/mol)
30 ^oC	40 ^oC	50 ^oC	60 ^oC		
-1.607	-2.496	-3.752	-4.708	0.105	30.406

The presence of negative values for ΔG^o signifies the natural spontaneity of the sorption process. The positive value of ΔH^o suggests the endothermic nature of the adsorption process. The entropy change has a positive sign, which reveals that the randomness at the interface of solid and liquid will increase during the adsorption of CIP [42].

7. Conclusion

In the present study, the conversion of tea residue into activated carbon was accomplished, followed by its utilization for the efficient adsorption of Ciprofloxacin from an aqueous solution. The optimal conditions for the adsorption process, resulting in a maximum removal efficiency of 94.4% for Ciprofloxacin, are as follows: a mixing time of 454 minutes, an acidity pH of 8.75, a dosage of 0.194 g/25 ml of aqueous solution, and an initial Ciprofloxacin concentration of 200 ppm. The BET analysis of the prepared activated carbon shows a surface area value of 774 m^2/g and 0.563 cm^3/g, respectively. The adsorption of Ciprofloxacin on the active carbon that was synthesized may be effectively described using the Langmuir model, which precisely predicts the equilibrium adsorption behavior. The Langmuir model indicates a maximum adsorption capacity of 256.41 mg/g. The adsorption kinetics and reaction rate constant K_2 in the pseudo-second-order model are characterized by a value of 0.001 g/ (mg. min). The thermodynamic analysis reveals that the adsorption of ciprofloxacin on tea-activated carbon is both endothermic and spontaneous.

Acknowledgment

We appreciate the help of the lab staff from the Al-Khwarizmi College of Engineering's Biochemical Engineering Department in carrying out various research-related laboratory tests. We would also like to express our gratitude to the Ministry of Health for providing us with Ciprofloxacin.

References

[1] S. D. Salman, "Adsorption of Heavy Metals from Aqueous Solution onto Sawdust Activated Carbon," *Al-Khwarizmi Engineering Journal*, vol. 15, no. 3, pp. 60–69, 2019.

[2] G. M. Abd-Hadi and S. D. Salman, "Adsorption of Para Nitro-phenol by Activated Carbon produced from Alhagi," *Sains Malaysiana*, vol. 49, no. 1, pp. 57–67, 2020, doi: 10.17576/jsm-2020-4901-07.

[3] M. M. H. Hammad, K. W. Hameed, and H. A. Sabti, "Reducing the Pollutants from Municipal Wastewater by Chlorella Vulgaris Microalgae," *Al-Khwarizmi Engineering Journal*, vol. 15, no. 1, pp. 97–108, 2019, doi:

10.22153/kej.2019.09.001.

[4] I. M. Rashid, A. I. Alwared, and H. N. Abdelkareem, "Biosorption of Cd (II) Ions by Chlorella Microalgae : Isotherm, Kinetics Processes, and Biodiesel Production," *Desalination and Water Treatment*, vol. 311, pp. 67–75, 2023, doi: 10.5004/dwt.2023.29990.

[5] I. M. Rashid, S. D. Salman, and A. K. Mohammed, "Removal of pathogenic bacteria from synthetic contaminated water using packed bed silver nanoparticle-coated substrates," *Energy, Ecology and Environment*, vol. 6, no. 5, pp. 462–468, Oct. 2021, doi: 10.1007/s40974-021-00208-3.

[6] R. Beksissa, B. Tekola, T. Ayala, and B. Dame, "Investigation of the adsorption performance of acid treated lignite coal for Cr (VI) removal from aqueous solution," vol. 4, no. December 2020, 2021, doi: 10.1016/j.envc.2021.100091.

[7] S. D. Salman, I. M. Rasheed, and M. M. Ismaeel, "Removal of diclofenac from aqueous solution on apricot seeds activated carbon synthesized by pyro carbonic acid microwave," *Chemical Data Collections*, vol. 43, no. December 2022, p. 100982, Feb. 2023, doi: 10.1016/J.CDC.2022.100982.

[8] L. Qalyoubi, A. Al-Othman, and S. Al-Asheh, "Removal of ciprofloxacin antibiotic pollutants from wastewater using nano-composite adsorptive membranes," *Environmental Research*, vol. 215, p. 114182, Dec. 2022, doi: 10.1016/J.ENVRES.2022.114182.

[9] J. Ma, M. Yang, F. Yu, and J. Zheng, "Water-enhanced Removal of Ciprofloxacin from Water by Porous Graphene Hydrogel," *Scientific Reports*, vol. 5, pp. 1–10, 2015, doi: 10.1038/srep13578.

[10] S. Cheikh *et al.*, "Complete Elimination of the Ciprofloxacin Antibiotic from Water by the Combination of Adsorption–Photocatalysis Process Using Natural Hydroxyapatite and TiO2," *Catalysts*, vol. 13, no. 2, 2023, doi: 10.3390/catal13020336.

[11] D. Hu and L. Wang, "Adsorption of ciprofloxacin from aqueous solutions onto cationic and anionic flax noil cellulose," *Desalination and Water Treatment*, vol. 57, no. 58, pp. 28436–28449, 2016, doi: 10.1080/19443994.2016.1183232.

[12] W. T. Jiang *et al.*, "Removal of ciprofloxacin from water by birnessite," *Journal of Hazardous Materials*, vol. 250–251, pp. 362–369, 2013, doi: 10.1016/j.jhazmat.2013.02.015.

[13] N. M. Jabbar, S. D. Salman, I. M. Rashid, and Y. S. Mahdi, "Removal of an anionic Eosin dye from aqueous solution using modified activated carbon prepared from date palm fronds," *Chemical Data Collections*, vol. 42, no. October, p. 100965, 2022, doi: 10.1016/j.cdc.2022.100965.

[14] W. Peng, H. Li, Y. Liu, and S. Song, "A review on heavy metal ions adsorption from water by graphene oxide and its composites," *Journal of Molecular Liquids*, vol. 230, pp. 496–504, 2017, doi: 10.1016/j.molliq.2017.01.064.

[15] J. Tao, X. Fu, C. Du, and D. Zhang, "Tea Residue-Based Activated Carbon: Preparation, Characterization and Adsorption Performance of o-Cresol," *Arabian Journal for Science and Engineering*, vol. 46, no. 7, pp. 6243–6258, 2021, doi: 10.1007/s13369-020-04968-8.

[16] A. Gundogdu, H. B. Senturk, C. Duran, M. Imamoglu, and M. Soylak, "A new low-cost activated carbon produced from tea-industry waste for removal of Cu (II) ions from aqueous solution : Equilibrium, kinetic and thermodynamic evaluation," *Karadeniz Chemical Science and Technology*, vol. 2, no. Ii, pp. 1–10, 2018.

[17] A. O. Egbedina, C. G. Ugwuja, P. A. Dare, H. D. Sulaiman, B. I. Olu-Owolabi, and K. O. Adebowale, "CTAB-activated Carbon from Peanut Husks for the Removal of Antibiotics and Antibiotic-resistant Bacteria from Water," *Environmental Processes*, vol. 10, no. 2, pp. 1–20, Jun. 2023, doi: 10.1007/S40710-023-00636-9/METRICS.

[18] S. M. Kakom, N. M. Abdelmonem, I. M. Ismail, and A. A. Refaat, "Activated Carbon from Sugarcane Bagasse Pyrolysis for Heavy Metals Adsorption," *Sugar Tech*, vol. 25, no. 3, pp. 619–629, 2023, doi: 10.1007/s12355-022-01214-3.

[19] A. L. Cazetta *et al.*, "NaOH-activated carbon of high surface area produced from coconut shell: Kinetics and equilibrium studies from the methylene blue adsorption," *Chemical Engineering Journal*, vol. 174, no. 1, pp. 117–125, 2011, doi: 10.1016/j.cej.2011.08.058.

[20] S. Wong, Y. Lee, N. Ngadi, I. M. Inuwa, and N. B. Mohamed, "Synthesis of activated carbon from spent tea leaves for aspirin removal," *Chinese Journal of Chemical Engineering*, vol. 26, no. 5, pp. 1003–1011, 2018, doi: 10.1016/j.cjche.2017.11.004.

[21] E. V. Liakos, K. Rekos, D. A. Giannakoudakis, A. C. Mitropoulos, J. Fu, and G. Z. Kyzas, "Activated porous carbon derived from tea and plane tree leaves biomass

for the removal of pharmaceutical compounds from wastewaters," *Antibiotics*, vol. 10, no. 1, pp. 1–16, 2021, doi: 10.3390/antibiotics10010065.

[22] A. K. A. K. Mohammed, H. F. H. F. Hameed, and I. M. I. M. Rashid, "Wastewater remediation using activated carbon derived from Alhagi plant," *Desalination and Water Treatment*, vol. 300, pp. 36–43, 2023, doi: 10.5004/dwt.2023.29706.

[23] A. El Nemr, R. M. Aboughaly, A. El Sikaily, M. S. Masoud, M. S. Ramadan, and S. Ragab, "Microporous-activated carbons of type I adsorption isotherm derived from sugarcane bagasse impregnated with zinc chloride," *Carbon Letters*, vol. 32, no. 1, pp. 229–249, 2022, doi: 10.1007/s42823-021-00270-1.

[24] R. Zakaria, N. A. Jamalluddin, and M. Z. Abu Bakar, "Effect of impregnation ratio and activation temperature on the yield and adsorption performance of mangrove-based activated carbon for methylene blue removal," *Results in Materials*, vol. 10, no. April, p. 100183, 2021, doi: 10.1016/j.rinma.2021.100183.

[25] O. Üner and Y. Bayrak, "The effect of carbonization temperature, carbonization time and impregnation ratio on the properties of activated carbon produced from Arundo donax," *Microporous and Mesoporous Materials*, vol. 268, pp. 225–234, 2018, doi: 10.1016/j.micromeso.2018.04.037.

[26] K. E. Talib and S. D. Salman, "Removal of Malachite Green from Aqueous Solution using Ficus Benjamina Activated Carbon-Nonmetal Oxide synthesized by pyro Carbonic Acid Microwave," *Al-Khwarizmi Engineering Journal*, vol. 19, no. 2, pp. 26–38, 2023, doi: 10.22153/kej.2023.03.002.

[27] M. H. Al-Hassani, "Al-Khriet Agricultural Waste Adsorbent, for Removal Lead and Cadmium Ion from Aqueous Solutions," *Al-Khwarizmi Engineering Journal*, vol. 9, no. 2, pp. 69–76, 2013.

[28] N. Jabbar, A. Mohammed, and E. Kadhim, "Biodegradation of Diesel Contaminated Soil Using Single Bacterial Strains and a Mixed Bacterial Consortium," *Al-Khwarizmi Engineering Journal*, vol. 13, no. 4, pp. 80–88, 2017.

[29] S. M. Yakout and G. Sharaf El-Deen, "Characterization of activated carbon prepared by phosphoric acid activation of olive stones," *Arabian Journal of Chemistry*, vol. 9, pp. S1155–S1162, 2016, doi: 10.1016/j.arabjc.2011.12.002.

[30] M. Zięzio, B. Charmas, K. Jedynak, M. Hawryluk, and K. Kucio, "Preparation and characterization of activated carbons obtained from the waste materials impregnated with phosphoric acid(V)," *Applied Nanoscience (Switzerland)*, vol. 10, no. 12, pp. 4703–4716, 2020, doi: 10.1007/s13204-020-01419-6.

[31] Y. El Maguana and N. Elhadiri, "Optimization of preparation conditions of activated carbon from walnut cake using response surface methodology .," vol. 23, no. November 2020, pp. 147–150, 2018.

[32] F. J. Tuli, A. Hossain, A. K. M. F. Kibria, A. R. M. Tareq, S. M. M. A. Mamun, and A. K. M. A. Ullah, "Removal of methylene blue from water by low-cost activated carbon prepared from tea waste: A study of adsorption isotherm and kinetics," *Environmental Nanotechnology, Monitoring and Management*, vol. 14, no. July, p. 100354, 2020, doi: 10.1016/j.enmm.2020.100354.

[33] H. Zhu, T. Chen, J. Liu, and D. Li, "Adsorption of tetracycline antibiotics from an aqueous solution onto graphene oxide/calcium alginate composite fibers," *RSC Advances*, vol. 8, no. 5, pp. 2616–2621, 2018, doi: 10.1039/c7ra11964j.

[34] B. Bhattarai and R. P. S. Suri, "Environmentally Friendly β - Cyclodextrin − Ionic Liquid Polyurethane- Modi fi ed Magnetic Sorbent for the Removal of PFOA, PFOS, and Cr(VI) from Water," no. Vi, 2017, doi: 10.1021/acssuschemeng.7b02186.

[35] B. B. Saha, S. Jribi, S. Koyama, and I. I. El-Sharkawy, "Carbon dioxide adsorption isotherms on activated carbons," *Journal of Chemical and Engineering Data*, vol. 56, no. 5, pp. 1974–1981, 2011, doi: 10.1021/je100973t.

[36] B. Li, Q. Zhang, and C. Ma, "Kinetics of SO2Adsorption on Powder Activated Carbon in a Drop Tube Furnace," *International Journal of Chemical Engineering*, vol. 2021, 2021, doi: 10.1155/2021/8886646.

[37] Arnelli, W. P. Aditama, Z. Fikriani, and Y. Astuti, "Adsorption kinetics of surfactants on activated carbon," *IOP Conference Series: Materials Science and Engineering*, vol. 349, no. 1, 2018, doi: 10.1088/1757-899X/349/1/012001.

[38] H. Moussout, H. Ahlafi, M. Aazza, and H. Maghat, "Critical of linear and nonlinear equations of pseudo-first order and pseudo-second order kinetic models," *Karbala International Journal of Modern Science*, vol. 4, no. 2, pp. 244–254, 2018, doi:

10.1016/j.kijoms.2018.04.001.

[39] S. Raghav and D. Kumar, "Adsorption Equilibrium, Kinetics, and Thermodynamic Studies of Fluoride Adsorbed by Tetrametallic Oxide Adsorbent," *Journal of Chemical and Engineering Data*, vol. 63, no. 5, pp. 1682–1697, 2018, doi: 10.1021/acs.jced.8b00024.

[40] S. D. Salman and I. M. Rashid, "Production and characterization of composite activated carbon from potato peel waste for cyanide removal from aqueous solution," *Environmental Progress & Sustainable Energy*, p. e14260, Sep. 2023, doi: 10.1002/EP.14260.

[41] S. Mustapha, D. T. Shuaib, M. M. Ndamitso1, M. B. Etsuyankpa, A. Sumaila1, U. M. Mohammed, and M. B. Nasirudeen "Adsorption isotherm, kinetic and thermodynamic studies for the removal of Pb(II), Cd(II), Zn(II) and Cu(II) ions from aqueous solutions using Albizia lebbeck pods," *Applied Water Science*, vol. 9, no. 6, pp. 1–11, 2019, doi: 10.1007/s13201-019-1021-x.

[42] H. T. Fan, L. Q. Shi, H. Shen, X. Chen, and K. P. Xie, "Equilibrium, isotherm, kinetic and thermodynamic studies for removal of tetracycline antibiotics by adsorption onto hazelnut shell derived activated carbons from aqueous media," *RSC Advances*, vol. 6, no. 111, pp. 109983–109991, 2016, doi: 10.1039/c6ra23346e.

تعديل وتوصيف الكربون المنشط المحضر من بقايا الشاي وامتصاص سيبروفلوكساسين

علاء كريم محمد* **إسراء مزاحم رشيد**** **ناديا حسين السباني*****
وان نور رسلام وان عيسى****
*،***قسم الهندسة الكيميائية الاحيائية/ كلية الهندسة الخوارزمي/ جامعة بغداد*
*** قسم الهندسة الكيميائية/ كلية هندسة النفط والغاز/ جامعة الزاوية/ ليبيا*
**** قسم الهندسة الكيميائية وهندسة العمليات/ كلية الهندسة والبيئة / جامعة كيبانجسان/ ماليزيا*
*البريد الالكتروني:dr.alaa@kecbu.uobaghdad.edu.iq
**البريد الالكتروني:israa_msc2018@kecbu.uobaghdad.edu.iq
***البريد الالكتروني: n.alsbani@zu.edu.ly
****البريد الالكتروني:wannorroslam@ukm.edu.my

الخلاصة

تقدم هذه الدراسة وصفا للطريقة المستعملة في تحضير الكربون المنشط (AC) من بقايا الشاي. تم دراسة الخواص الفيزيائية والكيميائية وكفاءة الامتزاز للكربون المنشط المحضر. وقد تم إنتاج الكربون المنشط (AC)على مرحلتين: الاولى التنشيط باستعمال حامض الفوسفوريك (H_3PO_4) والثانية الكربنة عند درجة حرارة 450 درجة مئوية. استعمل الكربون المنشط لغرض امتصاص العقار الدوائي السيبروفلوكساسين (CIP). فقد تمت دراسة عدة عوامل تشغيلية بدرجة حرارة الغرفة لمعرفة تأثيرها في كفاءة الامتزاز. تشمل هذه العوامل التركيز الأولي لـ CIP الممتز، ومستوى الرقم الهيدروجيني، وزمن الامتزاز، وكمية المادة المازة. وتم اختبار خصائص الكربون المنشط باستعمال التحليل الطيفي للأشعة تحت الحمراء (FTIR)، والمجهر الماسح الإلكتروني (SEM)، وحيود الأشعة السينية (XRD)، وحساب المساحة السطحية والحجم المسامي بطريقة (BET) . وتمت دراسة نمط الامتزاز وتبين ان نموذج Langmuir هو الموديل المناسب لعملية امتزاز CIP على الكربون المنشط بالشاي (TAC). إذ يتمتع الكربون المنشط المنتج بالقدرة على امتصاص السيبروفلوكساسين، بقدرة امتصاص قصوى تبلغ 256.41 ملغم/غرام. وقد تمت دراسة حركية الامتزاز وتبين انه يمكن تمثيلها بتفاعل من الدرجة الثانية.